Tracer development for detection and characterization of neuroendocrine tumors with PET

Neels, Olivier Christiaan

Chapter 3
Manipulation of [^{11}C]HTP and [^{18}F]FDOPA accumulation in neuroendocrine tumor cells

Oliver C. Neels[1], Klaas P. Koopmans[1], Pieter L. Jager[1], Laya Vercauteren[2], Aren van Waarde[1], Janine Doorduin[1], Hetty Timmer-Bosscha[3], Adrienne H. Brouwers[1], Elisabeth G.E. de Vries[3], Rudi A. Dierckx[1], Ido P. Kema[4], Philip H. Elsinga[1].

Departments of Nuclear Medicine and Molecular Imaging[1], Medical Oncology[3] and Pathology and Laboratory Medicine[4], University of Groningen and University Medical Center Groningen, The Netherlands
Department of Pharmacy[2], University of Ghent, Belgium

Submitted for publication.

Summary

[^{11}C]-5-Hydroxytryptophan ([^{11}C]HTP) and 6-[^{18}F]fluoro-levodopa ([^{18}F]FDOPA) are used to image neuroendocrine tumors (NETs) with positron emission tomography (PET). The precise mechanism by which these tracers accumulate in tumor cells is unknown. We aimed to study tracer uptake via large amino acid transporters (LAT), peripheral decarboxylation (inhibited by carbidopa) and intracellular breakdown by monoamine oxidase (MAO). [^{11}C]HTP and [^{18}F]FDOPA tracer accumulation was assessed in a human neuroendocrine tumor cell line BON. The carbidopa experiments were performed in a tumor bearing mouse model. Intracellular [^{11}C]HTP accumulation was 2-fold higher than [^{18}F]FDOPA. Cellular transport of both tracers was inhibited by amino-2-norbornanecarboxylic acid. The MAO inhibitors clorgyline and pargyline increased tracer accumulation *in vitro*. Carbidopa did not influence tracer accumulation *in vitro* but improved tumor imaging *in vivo*. Despite lower accumulation *in vitro*, visualization of [^{18}F]FDOPA is superior to [^{11}C]HTP in the neuroendocrine pancreatic tumor xenograft model. This could be a consequence of the serotonin saturation of BON cells in the *in vivo* model.

Introduction

Because of high sensitivity positron emission tomography (PET) studies for imaging of neuroendocrine tumors (NETs) have recently raised interest[1,2,3,4,5,6,7]. To visualize these tumors the principle of amine precursor uptake and decarboxylation (APUD)[8] and imaging of the somatostatin receptor plays a major role. Neuroendocrine tumors possess the unique property of synthesis, storage and secretion of biogenic amines. Clinically applied tracers to visualize this are 6-[^{18}F]fluoro-levodopa ([^{18}F]FDOPA) and [^{11}C]-5-hydroxytryptophan ([^{11}C]HTP).

Despite the clinical utility of these tracers, little is known about the precise mechanisms that govern their accumulation in tumor cells. Several factors are potentially involved in this accumulation. The first factor is the fact, as both tracers are amino acid derivatives, that they may well be a substrate for transmembrane amino acid transporters. The Na^+-independent transporters LAT1, LAT2, LAT3 and LAT4 are defined as system L transporters and can be blocked by the model substrate amino-2-norbornanecarboxylic acid (BCH)[9]. LAT transporters are responsible for the transport of large neutral amino acids across the cellular membrane.

Secondly, the precise effects of the peripheral decarboxylation inhibitor carbidopa, generally given to patients before [^{11}C]HTP or [^{18}F]FDOPA tracer injection in order to improve uptake, are poorly understood.

A third factor involved can be monoamine oxidase (MAO). It plays a major role in the metabolism of tryptophan and levodopa and is the enzyme responsible for the degradation of serotonin (5-HT) to 5-hydroxyindole acetic acid (5-HIAA) and of dopamine to homovanillic acid. Based on inhibitor sensitivity and substrate selectivity MAOs are subtyped as MAO A and B[10,11]. While MAO A is mainly responsible for the degradation of 5-HT, MAO B breaks down both 5-HT and dopamine[12]. With the use of selective and non-selective MAO inhibitors like clorgyline (MAO A) and pargyline (MAO A & B) the effect of the MAOs on tracer trapping can be examined[13,14]. An increased accumulation due to reduced intracellular metabolism of [^{11}C]HTP and [^{18}F]FDOPA can be expected by the use of MAO inhibitors.

The aim of the present study was the analysis of the uptake of [^{11}C]HTP and [^{18}F]FDOPA by large amino acid transporters (LAT), peripheral decarboxylation by amino acid decarboxylase (AADC) and intracellular breakdown by monoamine oxidase (MAO) *in vitro*. Finally, experiments with carbidopa were extended to a tumor-bearing animal model to get a better understanding of the *in vivo* metabolism, using microPET.

Materials and Methods

Materials

Tracers

Synthesis of [^{18}F]FDOPA was carried out as described earlier[15] with an average specific activity of 9.8 GBq/mmol after end of synthesis. The tracer was diluted with 0.9 % saline to the required concentration of ~ 1 MBq/ml. 0.19 ± 0.01 ml [^{18}F]FDOPA corresponding to a dose of 6.17 ± 0.63 MBq was injected per animal. [^{11}C]HTP was synthesized via an enzymatic method with an average specific activity of 30,000 GBq/mmol after end of synthesis as recently described[16]. It was used at a concentration of ~ 20 MBq / ml. 0.24 ± 0.02 ml [^{11}C]HTP, corresponding to a dose of 10.79 ± 1.18 MBq were injected per animal.

Chemicals

5-HTP, 5-HT, 5-HIAA, carbidopa, clorgyline, pargyline hydrochloride and BCH were purchased from Sigma (Zwijndrecht, The Netherlands). GMC (5.6 mM *D*-glucose, 0.49 mM $MgCl_2$, 0.68 mM $CaCl_2$) was added to phosphate-buffered saline solution (PBS; 140 mM NaCl, 2.7 mM KCl, 6.4 mM Na_2HPO_4, 0.2 mM KH_2PO_4). pH of the resulting PBS-GMC solutions was adjusted to 7.4 with sodium hydroxide. PBS-GMC was used to deplete internal amino acid pools[17,18]. Matrigel was purchased from BD Biosciences (Erembodegem, Belgium).

In vitro experiments

Cell culture method

Experiments were performed with the human neuroendocrine pancreatic tumor cell line BON[19]. Cells were maintained in 25 cm^2 culture flasks in 5 ml D-MEM/F-12 (1:1) medium supplemented with 10 % fetal calf serum (FCS) containing the amino acids *L*-phenylalanine (215 µmol) and *L*-tryptophan (44 µmol) amongst others. Cells were grown in a humidified atmosphere containing 5 % CO_2 and were routinely subcultured every 3-4 days. Cultures grown to a cell density of 1.0 x 10^6 - 1.4 x 10^6 cells per ml were used for experiments.

Cells were harvested by trypsin treatment, resuspended and diluted 3:7 in culture medium on 12 wells plates 1 day before the experiments (1 ml per well). Viability and number of cells were determined by the trypan blue exclusion technique. Cell viability 1-2 hours after experiments was over 90 %. At the day of experiment, cells were washed with warm PBS (3 x 2 ml) and 1 ml of culture medium or PBS-GMC buffer per well was added. The cells were then placed in a water bath for 1 hour at 37°C before start of the experiments to allow depletion of internal amino acids. Accumulation experiments were started by addition of 150 µl [^{18}F]FDOPA (~ 0.2 MBq) or 60 µl [^{11}C]HTP (~ 1.2 MBq) of the solution in each well.

Determination of intracellular tracer accumulation
After completion of the experiment, buffer was removed and cells were washed with ice-cold PBS (3 x 2 ml) and harvested by addition of 200 µl trypsin per well. 1 ml growth medium per well was added, cells were resuspended, transferred to 10 ml tubes and counted in a gamma counter (Compugamma, LKB Wallac, Finland). Measurements of tracer accumulation were expressed as percentage of the radioactive dose per 1 x 10^5 cells. All results were corrected for non-specific accumulation. For the determination of non-specific tracer accumulation all washing procedures were done with ice-cold PBS. Experiments were performed in ice-cold culture medium or PBS-GMC buffer and wells-plates were placed on ice. Tracer accumulation at 0 °C was considered as non-specific binding. Results represent the mean of 3-4 experiments ± standard error of the mean. Individual experiments were performed in duplicate.

Inhibition experiments
Various concentrations of the blocking agent BCH (0-20 mM) were applied to determine an adequate blocking concentration. To maintain cell viability carbidopa was used at a maximum concentration of 0.08 mM as higher concentrations of carbidopa induced apoptosis. Clorgyline and pargyline were added in a concentration of 0.1 mM[20,21]. Inhibition experiments were carried out by adding 1 ml of culture medium (control and carbidopa only) or PBS-GMC containing the blocking agent in the relevant concentration to each well. Afterwards cells were incubated for 1 hour in order to achieve the required amino acid depletion. Subsequently, tracer incubation was performed and intracellular accumulation determined as described above. A tracer incubation time of 15 minutes was used for the blocking agent BCH. Tracer incubation times ranging of 5-60 minutes with AADC and MAO inhibitors carbidopa, clorgyline and pargyline were used. Due to the short half-life of ^{11}C, incubation periods longer than 60 minutes were not applied.

Non-labeled tracer accumulation
Because of the short half-life of PET isotopes the detection and quantification of radioactive 5-HTP metabolites like 5-HT or 5-HIAA is limited. A sensitive automatic detection method of 5-HTP and its metabolites used in carcinoid patients was used for the detection of non-labeled tracer *in vitro*[22]. For these experiments culture medium was removed from the 25 cm^2 culture flasks. Cells were then washed with PBS (3 x 2 ml). 5 ml PBS-GMC buffer containing the carbidopa (0.08 mM), the MAO A inhibitor clorgyline (0.1 mM) or the non-selective MAO inhibitor pargyline (0.1 mM) was added. After the 1 hour depletion period, non radioactive labeled 5-HTP (55 nM) was added in 5 ml PBS-GMC buffer.
After 15 and 60 minutes of tracer incubation, PBS-GMC buffer was removed. The buffer supernatant was analyzed for the amounts of 5-HIAA. Pre concentration was performed by liquid liquid extraction in the following way. Per sample 2 drops of glacial acetic acid, 1 g NaCl, 5 ml diethyl ether were added and slightly shaken. After centrifugation at 2,000 g for 5 minutes the organic phase was transferred into a test-tube and diethyl ether evaporated in a slight stream of nitrogen. Samples were dissolved in eluent and analyzed as described earlier[22].

For the analysis of 5-HTP metabolites supernatant was removed, the cells were harvested with 1 ml trypsin and resuspended in 1 ml PBS containing 10 % FCS. Cells were washed three times with ice-cold PBS (1 ml) and centrifuged for 10 minutes at 10,000 g. Cells were lysed using liquid nitrogen. The concentrations of 5-HTP, 5-HT and 5-HIAA present in the lysed BON cells dissolved in 1 ml saline were determined by the method described above. Cellular accumulation of non-labeled tracer was defined as amount of substance detected in lysed cells divided by the total amount of 5-HTP in incubation medium at the start of the experiment. All results were represented using the mean of 3 experiments ± standard error of the mean.

In vivo experiments

Animals

Nude male mice (BALB/c, age 6-8 weeks, body weight 18 to 24 grams) were obtained from Harlan Netherlands BV (Horst, The Netherlands). Experimental groups consisted of 4-5 animals to perform microPET scanning after injection of [^{11}C]HTP and [^{18}F]FDOPA. The total number of studied animals was 36. Animals were housed in temperature and humidity controlled rooms with 12-hours day and 12-hours night cycles and were provided with forage and water ad libitum. Animals were housed in hepa-filtered cages in the animal research facility of the University Medical Center Groningen under controlled water, lab chow, humidity and temperature conditions. At least 2 hours before starting experiments the animals were acclimated to laboratory conditions. All animal experiments were performed by licensed investigators in compliance with the Law on Animal Experiments of The Netherlands. The study protocol was approved by the Committee on Animal Ethics of the University of Groningen.

MicroPET scanning

60 minutes dynamic scanning followed by 10 minutes transmission scanning was performed using a Concorde microPET Focus 220 system equipped with microPET manager for data acquisition in list mode and ASIPro for preparing sinograms and image reconstruction. Using ASIPro's clipping tool, areas with very high activity that were not relevant to the current study, such as the liver region, were removed as to yield a more cleaned up version of the scan that is, therefore, easier to evaluate. Ordered subset expectation maximization (OSEM2D) statistics was applied for the quantitative analysis. The PET acquisition data were fully corrected for dead time, random coincidences, attenuation and scatter. PET image size was 128 x 128 x 95 voxels.

In all experiments, cells were harvested with trypsin and resuspended in 1 ml growth medium/matrigel 1:1 and injected subcutaneously (SC, 1 x 10^6 cells/injection) into the right shoulder of the animals to establish tumors. Growth of tumors was checked three times a week. After approximately 3 weeks growth, a 10 mm tumor size was reached and considered suitable for experiments. Intravenous (IV) injection and scanning procedure were performed under isoflurane anesthesia. 4-5 animals from each group received carbidopa (1 mg/kg) intraperitoneally (IP) in the abdominal region 1 hour before tracer injection. Thereafter, radioactive tracers ([^{11}C]HTP: 0.50 ± 0.24 MBq/g bodyweight; [^{18}F]FDOPA: 0.29 ± 0.13 MBq/g bodyweight) were injected IP in the abdominal region or IV via the penile vein. After scanning for 70 minutes (60 minutes dynamic scanning, 10

minutes transmission scan), animals were sacrificed to determine tracer accumulation in tumor tissue and in different body parts e.g. liver, kidney, pancreas, intestines, brain. Radioactivity was measured in a gamma counter. Measurements of tracer accumulation were expressed as percentage of the injected dose/g bodyweight.

Statistics
Differences between various groups were tested for statistical significance using Student's t-test for independent samples. P-values < 0.05 were considered significant.

Results

In vitro experiments

Time-course of tracer accumulation
Cellular accumulation of [^{18}F]FDOPA and [^{11}C]HTP of cells incubated in culture medium over a period of 60 minutes was rapid, but low ([^{18}F]FDOPA 0.07 ± 0.01 %, [^{11}C]HTP 0.15 ± 0.01 %/10^5 cells). However, in amino acid free PBS-GMC buffer both tracers showed very rapid accumulation and under these conditions considerably higher levels of accumulation were reached. [^{18}F]FDOPA was accumulated to 1.2 ± 0.2 %/10^5 cells after 15 minutes and remained constant up to the end of the 60 minutes incubation period. [^{11}C]HTP accumulation was much higher than [^{18}F]FDOPA (ratio 5:1) with a maximum tracer accumulation of 5.3 ± 0.8 %/10^5 cells at 60 minutes (figure 1).

Inhibition experiments
Incubation of cells with carbidopa did not affect accumulation of both [^{11}C]HTP and [^{18}F]FDOPA after 60 minutes, neither in full culture medium nor in PBS-GMC buffer. Clorgyline preincubation led to significant higher accumulation compared to control for [^{11}C]HTP (14.2 ± 3.8 %/10^5 cells after 60 minutes) and [^{18}F]FDOPA (9.2 ± 2.9 %/10^5 cells after 60 minutes) in PBS-GMC buffer. With pargyline slightly higher accumulation compared to control was obtained for [^{18}F]FDOPA (3.7 ± 0.7 %/10^5 cells after 60 minutes) (figure 1). Accumulation experiments with BCH were performed at the time point of 15 minutes since [^{18}F]FDOPA reached a plateau phase of accumulation at 15 minutes in untreated BON cells. At 1.0 mM BCH, the accumulation of [^{18}F]FDOPA and [^{11}C]HTP was inhibited to levels of 0.43 ± 0.02%/10^5 cells ([^{18}F]FDOPA) and 0.22 ± 0.08 %/10^5 cells ([^{11}C]HTP) and suppressed at 20 mM BCH. The BCH IC_{50} value for [^{11}C]HTP is 0.12 mM (figure 2). The lowest used concentration of 0.03 mM BCH resulted in a reduction of tracer accumulation to 45 % compared to control for [^{18}F]FDOPA and a BCH IC_{50} value of 0.01 mM.

Non-labeled tracer accumulation
In BON cells (control) apart from 5-HTP both 5-HT and 5-HIAA were detected, 15 and 60 minutes after starting incubation. Only low cellular 5-HT levels (0.6 ± 0.1 % after 60 minutes) were found compared to 5-HTP (12.0 ± 0.0 % after 60 minutes) and 5-HIAA (11.9 ± 0.8 % after 60 minutes) levels. Treatment with carbidopa did neither increase 5-HTP (3.0 ± 0.9 % after 60 minutes) nor decrease cellular levels of 5-HT (3.0 ± 0.3 % after 60 minutes) or 5-HIAA (11.8 ± 1.4 % after 60 minutes). Clorgyline however increased 5-HT (18.4 ± 2.9 % after 60 minutes) and decreased 5-HIAA levels (0.9±0.0 % after 60

minutes). Similar results were obtained after pargyline treatment (5-HT: 29.3 ± 5.0 %, 5-HIAA: 2.4 ± 0.2 % after 60 minutes) (figure 3).

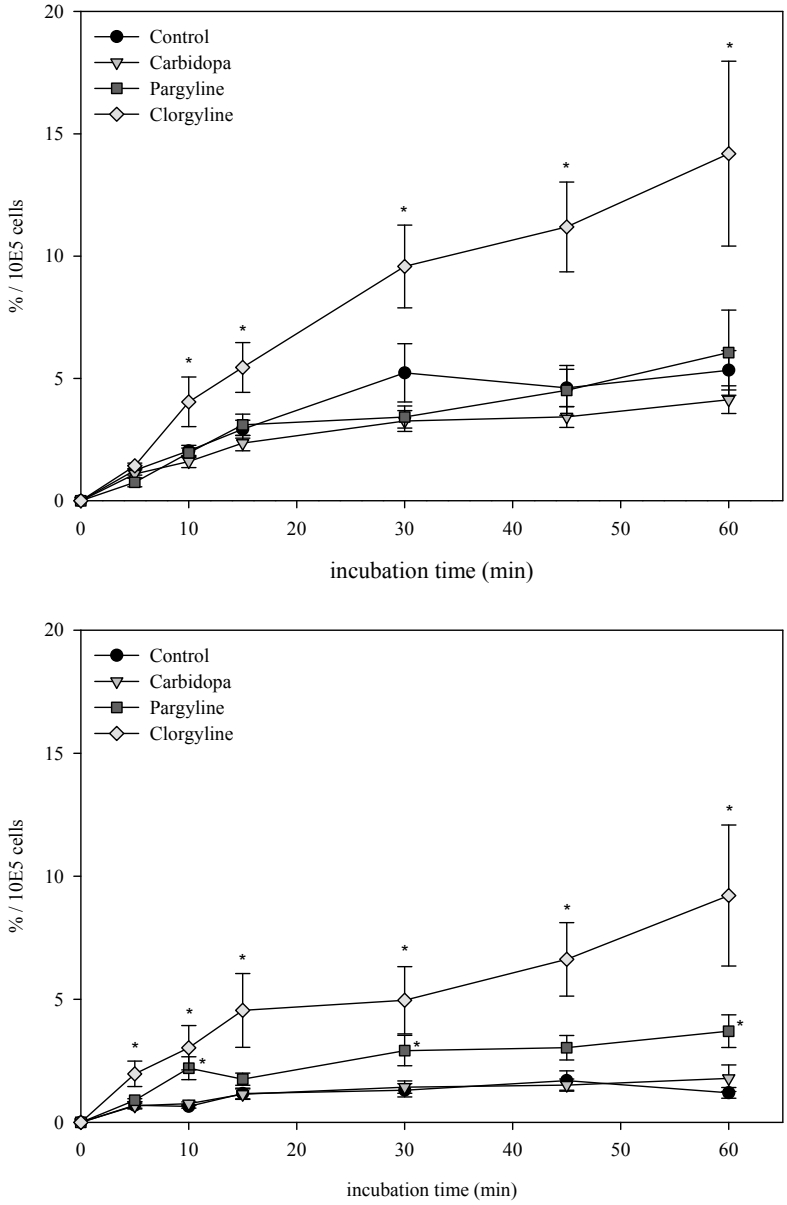

Figure 1. Accumulation of [^{11}C]HTP (top) and [^{18}F]FDOPA (bottom) in BON cells. Tracer accumulation was measured in amino acid free medium and was corrected for non-specific binding. Mean ± SEM of 3-4 experiments. *P≤0.05 compared to control.

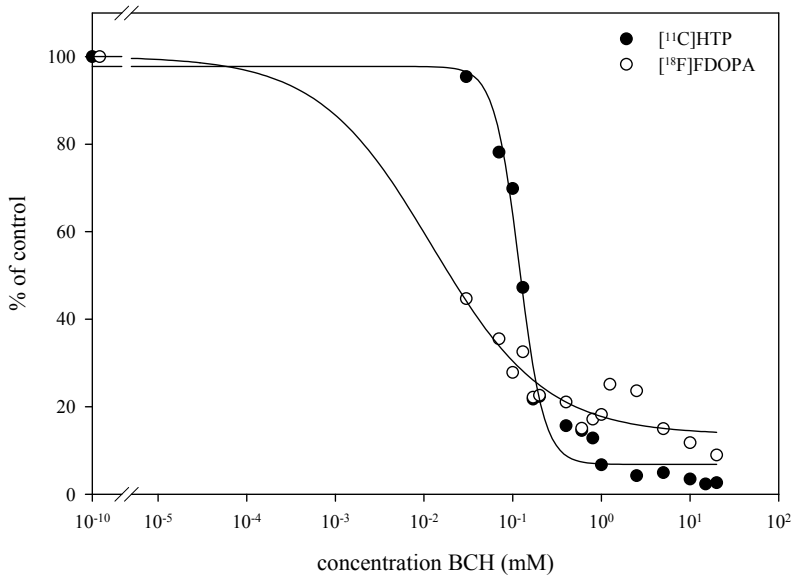

Figure 2. Accumulation of [^{11}C]HTP and [^{18}F]FDOPA in BON cells after inhibition of LAT. Tracer accumulation was measured in amino acid free medium and was corrected for non-specific binding. A concentration of 10^{-10} mM BCH is set as control. Incubation time: 15 minutes. Mean ± SEM of 3 experiments. BCH IC_{50} = 0.12 mM for [^{11}C]HTP, 0.01 mM for [^{18}F]FDOPA.

Animal experiments

36 mice were divided in 8 groups of 4-5 animals (control and carbidopa) and given [^{18}F]FDOPA or [^{11}C]HTP, IP or IV. In 33 of 36 mice microPET scans, tumors were visualized. Tumor weights on day of experiments ranged from 19 mg to 311 mg (average 118 mg) after decapitation. In 3 mice ([^{18}F]FDOPA IP control, [^{18}F]FDOPA IV carbidopa, [^{11}C]HTP IV carbidopa) scans, tumors were not visualized. In the tumor region following IV and IP administration [^{18}F]FDOPA in combination with carbidopa pretreatment gave the highest specific uptake values (SUVs) (figure 4). Within 5 minutes after IV tracer injection the plateau phase of the maximum tumor SUV for all experiments was reached except for [^{18}F]FDOPA combined with carbidopa given IP in the abdominal region. IP tracer injection showed increasing tumor SUV over time reaching a plateau phase later than 1 hour. Treatment with carbidopa resulted in higher SUVs for tumors compared to controls for both tracers within 60 minutes time. For IV injections both carbidopa treated and control, [^{18}F]FDOPA generated significant higher tumor SUVs than those obtained after [^{11}C]HTP. Biodistribution data after scanning demonstrated high SUVs for liver, kidney and pancreas for both tracers (IV). SUVs were not significantly altered after carbidopa treatment compared to control (figure 5). Although tumor SUVs in microPET images were higher for [^{18}F]FDOPA, [^{11}C]HTP resulted in higher uptake in most organs and significant differences in uptake were noted for spleen, red blood cells and blood plasma irrespective of carbidopa treatment.

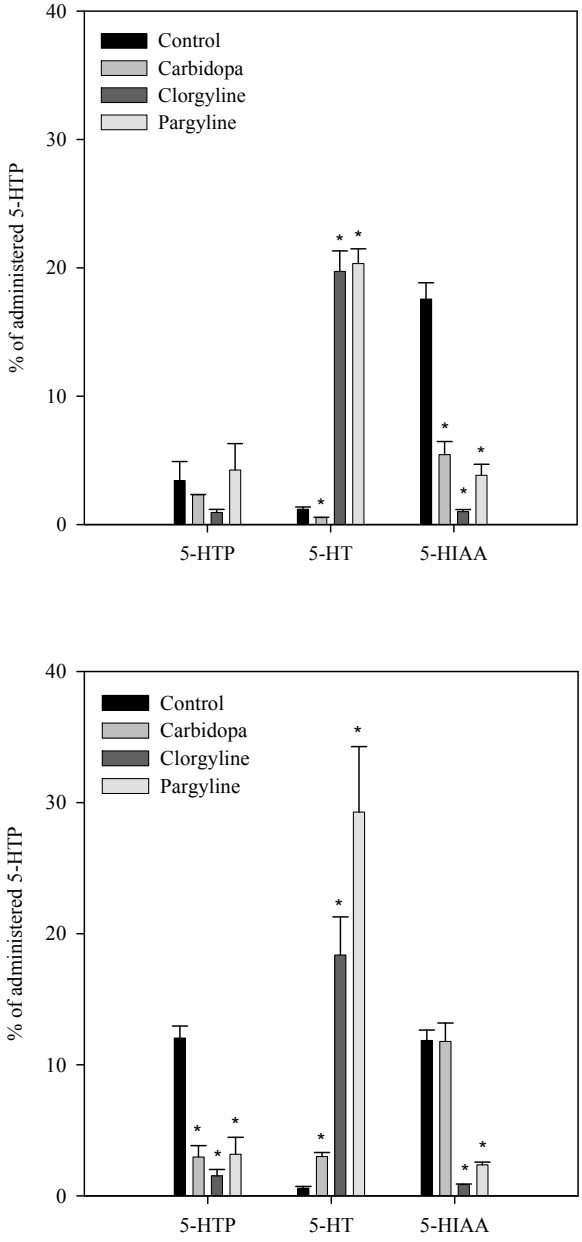

Figure 3. 5-HTP and metabolites in BON cells after incubation with 5-HTP. Top: 15 minutes incubation time. Bottom: 60 minutes incubation time. Mean ± SEM of 3 experiments. *P≤0.05 compared to control.

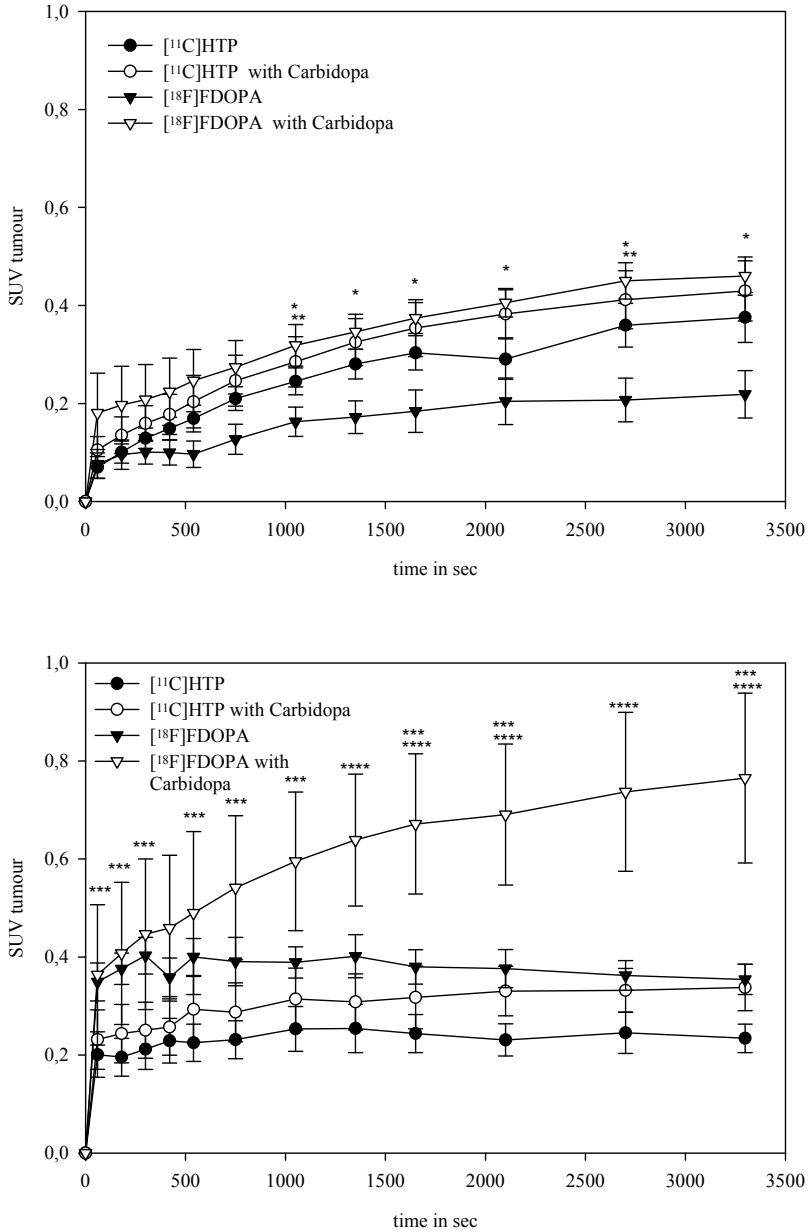

Figure 4. Tracer accumulation in tumor after IP (top) and IV (bottom) injection expressed as SUV. Graphics represent mean ± SEM of 4-5 animals. $P \leq 0.05$: *[^{18}F]FDOPA: Carbidopa vs. control, **Control: [^{11}C]HTP vs. [^{18}F]FDOPA, ***Control: [^{18}F]FDOPA vs. [^{11}C]HTP, ****Carbidopa: [^{18}F]FDOPA vs. [^{11}C]HTP.

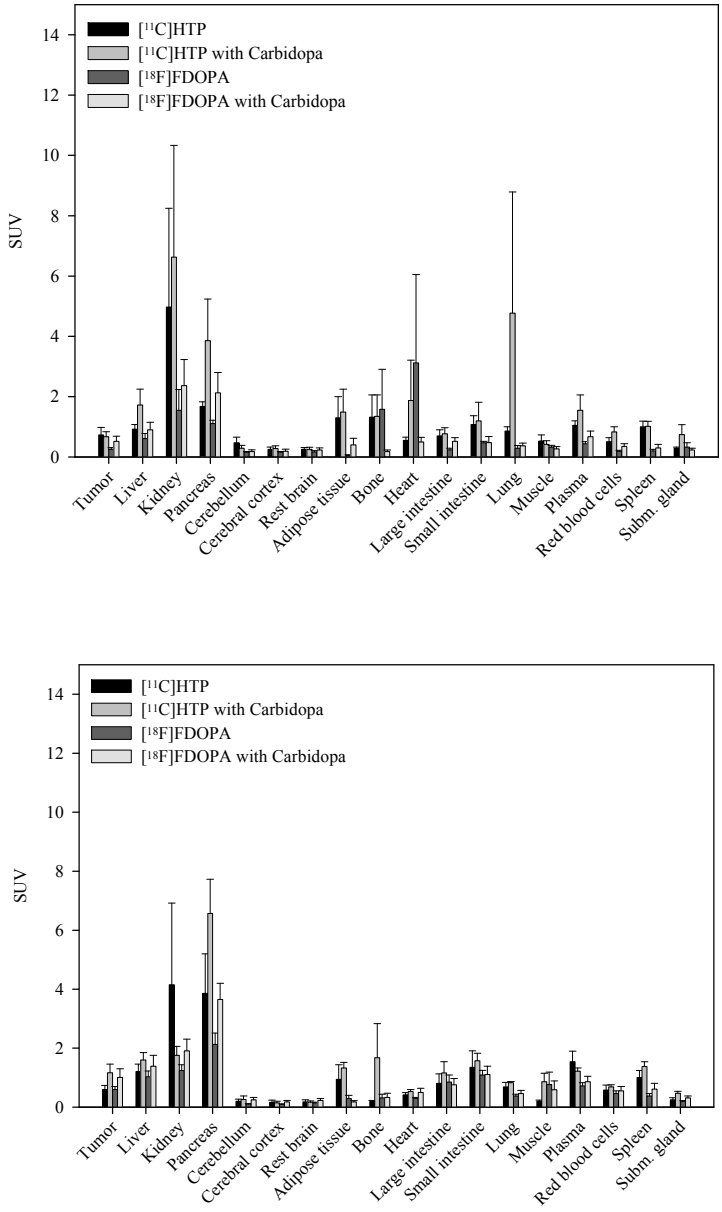

Figure 5. Accumulation of [11C]HTP and [18F]FDOPA in different organs 70 min after IP (top) and IV (bottom) injection, expressed as SUV. In separate experiments animals were pretreated with carbidopa. Values express mean ± SEM from 4-5animals.

Discussion

Cellular accumulation of [^{11}C]HTP and [^{18}F]FDOPA in neuroendocrine tumor cells is rapid and reaches a plateau after 15 minutes *in vitro* and within less than 5 minutes in the tumor in animal model after IV injection. We identified LAT, AADC and MAO as factors affecting intracellular tracer accumulation. Inhibition of amino acid transport resulted in a nearly complete shutdown of accumulation, illustrating that this mechanism is a key factor in intracellular accumulation. Carbidopa did not influence cellular accumulation of both tracers in tumor cells *in vitro* but did increase tumor accumulation of radioactivity in animals. *In vitro*, selective inhibition of MAO A by clorgyline induced increased accumulation of both tracers, confirming that MAO is a third important factor affecting their biodistribution. Non-selective inhibition of MAO by pargyline only increased [^{18}F]FDOPA accumulation.

We performed *in vitro* cellular accumulation experiments in culture medium because the levels of large amino acids as present in D-MEM/F-12 culture medium are similar to the ones in blood plasma[23]. The very low rates of [^{18}F]FDOPA and [^{11}C]HTP accumulation suggest that other amino acids in culture medium are competing for accumulation with these radiolabeled tracers. Thereafter the amino acid free PBS, in which cells remain viable during the 2 hours test period, was used. PBS was supplemented with *D*-glucose, magnesium chloride and calcium chloride as used by Jager *et al.*[18]. [^{11}C]HTP was accumulated twice as much as [^{18}F]FDOPA over a period of 60 minutes. This could be a consequence of the fact that BON cells produce more 5-HT than dopamine[24,25]. Retention of neurotransmitters is considered to be the resultant of uptake (LAT), decarboxylation (AADC) and granular storage by vesicular monoamine transporters (VMAT). The latter process prevents enzymatic breakdown in the cytoplasm (MAO) and subsequent secretion. One of the most important factors of VMAT activity is the amount of 5-HT or catecholamines in secretory vesicles[26,27]. In our cell studies the medium was free of amino acids and metabolites tentatively resulting in reduced filling of secretory granules. This theoretically led to higher VMAT-substrate activity. Separate granular storage of 5-HT and catecholamines and may explain differences in retention for [^{11}C]HTP and [^{18}F]FDOPA[28-30].

The cellular accumulation of [^{11}C]HTP and [^{18}F]FDOPA is blocked by low concentrations of BCH, a conventional inhibitor of the amino acid transporter system L[18]. An interesting aspect regarding the growth of BON tumor cells is its dependence on large amino acids. If the supply of those amino acids could be disrupted e.g. by BCH, proliferation would possibly be slowed down or stopped. Recently a dose-dependant inhibition of growth of C6 glioma cells was observed following BCH exposure *in vitro* and *in vivo*[22].

Örlefors *et al.* reported in patients an improved uptake of [^{11}C]HTP in carcinoid tumors and decreased urinary 5-HIAA levels when [^{11}C]HTP was administered after oral administration of carbidopa[31]. This was suggested to be the result of decreased conversion of [^{11}C]HTP and [^{18}F]FDOPA to [^{11}C]5-HT/[^{18}F]dopamine by activity of the AADC enzyme in peripheral tissues such as the liver and kidneys[32,33,34]. They hypothesized that the degradation of [^{11}C]HTP to [^{11}C]-5-HT in peripheral organs is blocked by carbidopa and thus increases the availability of [^{11}C]HTP resulting in higher accumulation of radiolabeled tracer in tumor lesions. Our results validate this hypothesis. Carbidopa did not affect the accumulation of [^{11}C]HTP or [^{18}F]FDOPA in BON cells. This suggests that intracellular

decarboxylation in BON cells was not inhibited. AADC activity was found to be upregulated in NET cells[36]. In nude mice bearing a BON tumor, carbidopa increased tracer tumor accumulation within the tumor resulting in better imaging (figure 6). Our mice PET images show high accumulation in the abdominal region. This is in line with our mice biodistribution data with high SUVs for organs such as liver and kidney located in this region. In the tumor model which we used, which was derived from a human pancreatic tumor cell line [^{18}F]FDOPA accumulation was higher than [^{11}C]HTP. Due to the high 5-HT production by carcinoid tumors[22], the granules in tumor cells of our animals are expected to be saturated with 5-HT. This may reduce granular storage of [^{11}C]-5-HT which results in cytoplasmic breakdown (MAO) and subsequent excretion of metabolites. As noted above, different granular storage of 5-HT and catecholamines may explain differences in tracer retention.

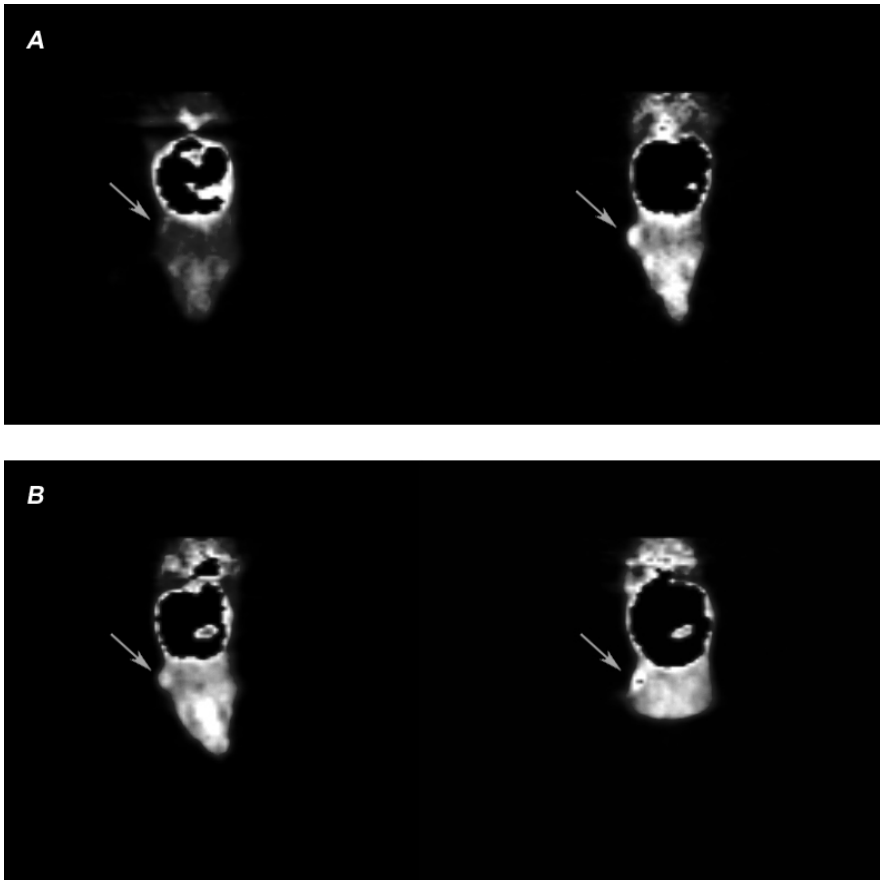

Figure 6. Full-color in appendix. A - [^{11}C]HTP PET after IV injection, coronal view. Left: control 22.6 g, 9.9 MBq, tumor weight 23.5 mg. Right: carbidopa treated 21.6 g, 6.2 MBq, tumor weight 61.1 mg. B - [^{18}F]FDOPA PET after IV injection, coronal view. Left: control 20.5 g, 8.4 MBq, tumor weight 109 mg. Right: carbidopa treated 23.6 g, 8.4 MBq, tumor weight 57.9 mg. Summed frames. Hot spots in abdominal region were cleaned up using ASIPro's clipping tool. Arrows point at tumors located in the right shoulder.

Increased *in vitro* accumulation was noticed after exposure to the MAO A inhibitor clorgyline. This result differs from reported PET studies with the MAO inhibitors harmine and deprenyl. Harmine and deprenyl both decreased the accumulation of [^{18}F]FDG and [^{11}C]DOPA in BON cells[37]. Degradation of [^{18}F]fluorodopamine and [^{11}C]-5-HT appears to be blocked by clorgyline. Pargyline gives a slightly higher [^{18}F]FDOPA accumulation compared to control in accordance with the fact that pargyline is an inhibitor for MAO B. Higher concentrations of pargyline could probably also lead to an increased [^{11}C]HTP accumulation.
In our institution, sensitive analytical methods to profile tryptophan related plasma indoles in patients[22] are available. This allowed us, as the half-life of ^{11}C is short, to determine the transformation of cold 5-HTP into 5-HT and 5-HIAA at 2 different time points (15 and 60 min) at equal concentrations as used for radioactive labeled [^{11}C]HTP. The use of selective AADC and MAO inhibitors gave insight into intracellular processes. Presence of AADC in BON cells is confirmed by the intracellular synthesis of 5-HT. No increase in 5-HTP is noticed after carbidopa treatment most likely as carbidopa is not a substrate for LAT transporters in BON cells and therefore not being transported into these cells. NET cells express upregulated AADC activity[36]. Inhibition of AADC will therefore not be inhibited by carbidopa within the tumor cell and intracellular conversion of 5-HTP into 5-HT will still be possible. Use of the MAO A inhibitor clorgyline and non-selective MAO inhibitor pargyline resulted in higher intracellular tumor 5-HT and lower 5-HIAA level. Once 5-HT is formed inside the cell, it appears not to be transported outside the cell before being deaminated by MAO into 5-HIAA.

Conclusion

Inhibition of LAT in BON cells leads to decreased tracer accumulation *in vitro*. Carbidopa does not influence tracer accumulation in tumor cells *in vitro* but improves tumor imaging *in vivo*. [^{18}F]FDOPA is superior to [^{11}C]HTP in tumor SUVs in this neuroendocrine pancreatic tumor xenograft model. MAO inhibition improves tracer accumulation *in vitro*.

Acknowledgements

BON cells were kindly provided by Dr. Ahlman from the Department of Surgery, Sahlgrenska University Hospital, Gothenburg, Sweden. We thank E.E.A. Venekamp and J. Krijnen for assistance in analyzing 5-HTP, 5-HT and 5-HIAA samples. This work was supported by grant 2003-2936 of the Dutch Cancer Society.

References

1. Rufini V, Calcagni ML, Baum RP. Imaging of neuroendocrine tumors. *Semin Nucl Med* 2006; **36**: 228-247.
2. Eriksson B, Örlefors H, Öberg K, Sundin A, Bergström M, Långström B. Developments in PET for the detection of endocrine tumours. *Best Pract Res Clin Endocrinol Metabol* 2005; **19**: 311-324.

3. Öberg K, Eriksson B. Nuclear medicine in the detection, staging and treatment of gastrointestinal carcinoid tumours. *Best Pract Res Clin Endocrinol Metabol* 2005; **19**: 265-276.
4. Örlefors H, Sundin A, Garske U, Juhlin C, Öberg K, Långström B, Bergström M, Eriksson B. Whole-body ^{11}C-5-hydroxytryptophan positron emission tomography as a universal imaging technique for neuroendocrine tumors – comparison with somatostatin receptor scintigraphy and computed tomography. *J Clin Endocrinol Metab* 2005; **90**: 3392-4000.
5. Montravers F, Grahek D, Kerrou K, Ruszniewski P, de Beco V, Aide N, Gutman F, Grangé JD, Talbot JN. Can fluorodihydroxyphenylalanine PET replace somatostatin receptor scintigraphy in patients with digestive endocrine tumors? *J Nucl Med* 2006; **47**: 1455-1462.
6. Koopmans KP, de Vries EGE, Kema IP, Elsinga PH, Neels OC, Sluiter WJ, van der Horst-Schrivers ANA, Jager PL. Staging of carcinoid tumours with ^{18}F-DOPA PET: a prospective, diagnostic study. *Lancet Oncol* 2006; **7**: 728-734.
7. Sundin A, Garske U, Örlefors H. Nuclear imaging of neuroendocrine tumors. *Best Pract. Res Clin Endocrinol Metab* 2007; **21**: 69-85.
8. Pearse AG. The APUD concept and hormone production. *Clin Endocrinol Metab* 1980; **9**: 211-22.
9. Fuchs BC, Bode BP. Amino acid transporters ASCT2 and LAT1 in cancer: partners in crime? *Sem Cancer Biol* 2005; **15**: 254-266.
10. Johnston JP. Some observations upon a new inhibitor of monoamine oxidase in brain tissue. *Biochem Pharmacol* 1968; **17**: 1285-1297.
11. Knoll J, Magyar K. Some puzzling effects of monoamine oxidase inhibitors. *Adv Biochem Psychopharmcol* 1972; **5**: 393-408.
12. Shih JC, Chen K, Ridd MJ. Monoamine oxidase: from genes to behavior. *Annu Rev Neurosci* 1999; **22**: 197-217.
13. Saura J, Kettler R, Da Prada M, Richards JG. Quantitative enzyme radioautography with ^{3}H-Ro 41-1049 and ^{3}H-Ro 19-6327 *in vitro*: localization and abundance of MAO-A and MAO-B in rat CNS, peripheral organs, and human brain. *J Neurosci* 1992; **12**: 1977-1999.
14. Saura J, Nadal E, van den Berg B, Vila M, Bombi JA, Mahy N. Localization of monoamine oxidase in human peripheral tissues. *Life Sci.* 1996; **59**: 1341-1349.
15. De Vries EFJ, Luurtsema G, Brussermann M, Elsinga PH, Vaalburg W. Fully automated synthesis module for the high yield one-pot preparation of 6-[^{18}F]fluoro-L-DOPA. *Appl Radiat Isot* 1999; **51**: 389–394.
16. Neels OC, Jager PL, Koopmans KP, Eriks E, de Vries EGE, Kema IP, Elsinga PH. Development of a reliable remote-controlled synthesis of β-[^{11}C]-5-hydroxy-*L*-tryptophan on a Zymark robotic system. *J Label Compd. Radiopharm* 2006; **49**: 889–895.
17. Shotwell MA, Jayme DW, Kilberg MS, Oxender DL. Neutral amino acid transport systems in chinese hamster ovary cells. *J Biol Chem* 1981; **256**: 5422-5427.
18. Jager PL, de Vries EGE, Piers DA, Timmer-Bosscha H. Uptake mechanisms of L-3-[^{125}I]iodo-alpha-methyl-tyrosine in a human small-cell lung cancer cell line: comparison with L-1-[^{14}C]tyrosine. *Nucl Med Comm* 2001; **22**: 87-96.

19. Evers BM, Townsend CM, Upp JR, Allen E, Hurlbut SC, Kim SW, Rajamaran S, Singh P, Reubi JC, Thompson JC. Establishment and characterization of a human carcinoid in nude mice and effect of various agents on tumor growth. *Gastroenterology* 1991; **101**: 303-311.
20. Pino R, Lyles GA. Effects of activity of semicarbazide-sensitive aminooxidases and cellular glutathione on the cytotoxic effect of allylamine, acrolein, and formaldehyde in human cultured endothelial cells. *Vopr Med Khim* 1997; **43**: 537-547.
21. Basma AN, Morris EJ, Nicklas WJ, Geller HM. L-DOPA cytotoxicity to PC12 cells in is via its autooxidation. *J Neurochem* 1995; **64** 825-832.
22. Kema IP, Meijer WG, Meiborg G, Ooms B, Willemse PHB, de Vries EGE. Profiling of tryptophan-related plasma indoles in patients with carcinoid tumors by automated, on-line, solid-phase extraction and HPLC with fluorescence detection. *Clin Chem* 2001; **47**: 1811-1820.
23. Hagberg GE, Torstenson R, Marteinsdottir I, Fredrikson M, Långström B, Blomqvist G. Kinetic compartment modeling of [^{11}C]-5-hydroxy-L-tryptophan for positron emission tomography assessment of serotonin synthesis in human brain. *J Cereb Blood Flow Metab* 2002; **22** 1352-1366.
24. Parekh D, Ishizuka J, Townsend CM, Haber B, Beauchamp RD, Karp G, Kim SW, Rajamaran S, Greeley G, Thompson JC. Characterization of a human pancreatic carcinoid in vitro: morphology, amine and peptide storage, and secretion. *Pancreas* 1994; **9**: 83-90.
25. Lemmer K, Ahnert-Hilger G, Höpfner M, Hoegerle S, Faiss S, Grabowski P, Jockers-Scherübl M, Riecken E, Zeitz M, Scherübl H. Expression of dopamine receptors and transporter in neuroendocrine gastrointestinal tumor cells. *Life Sci* 2002; **71**: 667-678.
26. Brunk B, Blex C, Rachakonda S, Höltje M, Winter S, Pahner I, Walther DJ, Ahnert-Hilger G. The first luminal domain of vesicular monoamine transporters mediates G-protein-dependent regulation of transmitter uptake. *J Biol Chem* 2006; **281**: 33373-33385.
27. Höltje M, Winter S, Walther D, Pahner I, Hörtnagl H, Ottersen OP, Bader M, Ahnert-Hilger G. The vesicular monoamine content regulates VMAT2 activity through $G\alpha_q$ in mouse platelets. *J Biol Chem* 2003; **278**: 15850-15858.
28. Feldman JM. Monoamine and dimonoamine oxidase activity in the diagnosis of carcinoid tumors. *Cancer* 1985, **56**: 2855-2860.
29. Smith CC. Evidence for separate serotonin and catecholamine compartments in human platelets. *Biochem Biophys Acta* 1996; **1291**: 1-4.
30. Eissele R, Anlauf M, Schärfer MKH, Eiden LE, Arnold R, Weihe E. Expression of vesicular monoamine transporters in endocrine hyperplasia and endocrine tumors of the oxyntic stomach. *Digestion* 1999; **60**: 428-439.
31. Örlefors H, Sundin A, Lu L, Öberg K, Långström B, Eriksson B, Bergström M. Carbidopa pretreatment improves image interpretation and visualisation of carcinoid tumours with ^{11}C-5-hydroxytryptophan positron emission tomography. *Eur J Nucl Med Mol Imaging* 2006; **33**: 60-65.

32. Hoffman JM, Melega WP, Hawk TC, Grafton SC, Luxen A, Mahoney DK, Barrio JR, Huang SC, Mazziotta. JC, Phelps ME. The effects of carbidopa administration on 6-[^{18}F]fluoro-L-DOPA kinetics in positron emission tomography. *J Nucl Med* 1992; **32**: 1472-1477.
33. Eriksson B, Bergström M, Örlefors H, Sundin A, Öberg K, Långström B. Use of PET in neuroendocrine tumors. *In vivo* applications and *in vitro* studies. *Q J Nucl Med* 2000; **44**: 68-76.
34. Bergström M, Lu L, Eriksson B, Marques M, Bjurling P, Andersson Y, Långström B. Modulation of organ uptake of ^{11}C-labelled 5-hydroxytryptohan. *Biogenic Amines* 1996; **12**: 477-485.
35. Nawashiro H, Otani N, Shinomiya N, Fukui S, Ooigawa H, Shima K, Matsuo H, Kanai Y, Endou H. L-type amino acid transporter 1 as a potential molecular target in human astrocytic tumors. *Int J Cancer* 2006; **119**: 484-492.
36. Vachtenheim J, Novotná H. Expression of the aromatic L-amino acid decarboxylase mRNA in human tumour cell lines of neuroendocrine and neuroectodermal origin. *Eur J Cancer* 1997; **33**: 2411-2417.
37. Xing T, Wu F, Brodin O, Fasth KJ, Långström B, Bergström M. *In vitro* PET evaluations in lung cancer cell Lines. *Anticancer Res* 2000; **20**: 1375-1380.